Euphorbia factor L2 suppresses the generation of liver metastatic ascites in breast cancer via inhibiting NLRP3 inflammasome activation

DONGJING JIANG[1], XUN LIU[1], RULAN TAN[1], YE ZHU[1] and LI ZHANG[2]

[1]Traditional Chinese Medicine and Research Office, Suzhou Vocational Health College, Suzhou, Jiangsu 215000; [2]Jiangsu Key Laboratory for High Technology Research of TCM Formulae, National and Local Collaborative Engineering Center of Chinese Medicinal Resources Industrialization and Formulae Innovative Medicine and Jiangsu Collaborative Innovation Center of Chinese Medicinal Resources Industrialization, Nanjing University of Chinese Medicine, Nanjing, Jiangsu 210023, P.R. China

Received April 13, 2023; Accepted November 14, 2023

DOI: 10.3892/ijmm.2023.5332

Abstract. Metastasis is the leading cause of death in patients with breast cancer, in part due to the lack of effective treatments. Euphorbia factor L2 (EFL2) is a diterpenoid extracted from *Euphorbia lathyris L.* seeds, which has attracted increasing attention in recent years due to its anticancer effect. However, the role and molecular mechanism of EFL2 in breast cancer liver metastasis remain unclear. In the present study, a breast cancer liver metastasis model was constructed and the effect of EFL2 on ascites generation in mice was examined. H&E staining detected inflammatory cells and tumor cells in the liver, small intestine and tumor tissues. Western blotting and reverse transcription-quantitative PCR were used to detect the protein and mRNA expression of NLR family pyrin domain containing-3 (NLRP3) and related molecules in tumor tissues. Immunohistochemistry was used to detect the levels of CD4 and CD8 T cells in tumor tissue and immunofluorescence was used to further detect the expression level of NLRP3. Finally, the aforementioned experiments were further verified by overexpressing NLPR3. It was found that EFL2 inhibited generation of ascites in the model in a dose-dependent manner. Furthermore, EFL2 inhibited tumor cell metastasis and enhanced immune cell infiltration. Meanwhile, EFL2 dose-dependently downregulated the mRNA and protein expression of NLRP3 and related molecules in the model, and overexpression of NLRP3 abolished these beneficial effects of EFL2. Taken together, the present experimental data suggested that EFL2 has a significant inhibitory effect on ascites of breast cancer liver metastasis *in vivo*, which may inhibit tumor cell metastasis by downregulating NLRP3 expression, providing an experimental basis for treating breast cancer metastasis.

Correspondence to: Dr Dongjing Jiang, Traditional Chinese Medicine and Research Office, Suzhou Vocational Health College, 28 Kehua Road, Suzhou, Jiangsu 215000, P.R. China
E-mail: jiangdongjing@szhct.edu.cn

Professor Li Zhang, Jiangsu Key Laboratory for High Technology Research of TCM Formulae, National and Local Collaborative Engineering Center of Chinese Medicinal Resources Industrialization and Formulae Innovative Medicine and Jiangsu Collaborative Innovation Center of Chinese Medicinal Resources Industrialization, Nanjing University of Chinese Medicine, 38 Xianlin Road, Nanjing, Jiangsu 210023, P.R. China
E-mail: zhangli@njucm.edu.cn

Key words: breast cancer, metastasis, ascites, Euphorbia factor L2, NLR family pyrin domain containing-3

Introduction

Breast cancer is the most common cancer in women worldwide. The International Agency for Research on Cancer (IARC) released GLOBOCAN 2018 statistics from 185 countries, which showed 2.3 million new cases (11.7%) and a 6.9% death rate from breast cancer (1). Despite a 39% drop in mortality over the past 30 years, it remains the leading cause of cancer-related death in women (2). A total of 5-11% of patients with breast cancer have metastases despite surgery, radiation, or chemotherapy (3). Breast cancer metastasis is the leading cause of death among women in numerous countries (4). Compared with other common metastatic sites, the liver is one of the most common sites of metastatic recurrence (5). As a common symptom in patients with liver metastases from breast cancer, ascites is associated with its progression. Malignant ascites (MA), a common clinical presentation in patients with advanced tumors, is a dire complication characterized by ascites and is associated with poor prognosis (6,7). MA is a very serious and difficult problem for patients with cancer and is one of the most common complications of advanced breast cancer. MA is known to create a pro-inflammatory environment that promotes immunosuppression and allows tumor cell proliferation and metastasis (8-10). Clearly, there is a need to identify new and effective treatments for metastatic breast cancer, and effective reduction of ascites in patients with breast cancer is critical for this.

Inflammation is one of the typical features of cancer and is a component of cancer initiation, progression and

metastasis (11). It is now considered a hallmark of cancer and an attractive target for cancer therapy. Numerous studies have shown that cancer metastasis is associated with inflammation (12). For instance, Shen *et al* (13) reported that inflammatory factors such as IL-1 and IL-6 can promote the expression of matrix metalloproteinases through NF-κB and STAT3, thereby inducing tumor cell invasion and metastasis, providing an explanation for the role of inflammation in cancer metastasis. In addition, inflammation is increasingly recognized as an important component of metastasis in breast cancer. Studies have identified that controlling cancer-induced inflammation prevents lung metastases in murine models of breast cancer (14) and inflammation triggered by loss of p53 drives breast cancer metastasis (15). Therefore, anti-inflammatory is expected to be an effective treatment for inhibiting breast cancer metastasis.

The nucleotide-binding domain, leucine-rich containing family, NLR family pyrin domain containing-3 (NLRP3) is the most studied and best characterized type of inflammasome (16). It is a sensor protein that binds to ASC and Pro-caspase-1 to form inflammasomes, activates caspase-1, and causes the proinflammatory cytokines interleukin-1β (IL-1β) and interleukin-18 (IL-18) synthesis and secretion (17). It has attracted the attention and great interest of numerous research groups due to its involvement in the development of various types of tumors (18). Although it was originally reported that the inflammasome inhibits tumor growth by activating the immune system (19), increasing evidence has demonstrated that the activation of the inflammasome leads to cancer cell growth and promotes the process of cancer metastasis. For example, Li *et al* (20) revealed that IL-1β treatment induced a significant increase in gastric cancer cell proliferation, while NLRP3 gene silencing significantly inhibited the growth of gastric cancer cells. Guo *et al* (21) reported that tumor growth and metastasis were significantly reduced in NLRP3 knockout mice in a breast cancer xenograft model. Similarly, Ershaid *et al* (22) investigated the correlation between NLRP3 inflammasome activation in fibroblast and its effect on breast cancer development and metastasis, and indicated an upregulation of the NLRP3 pathway for both murine mammary carcinogenesis and cancer-associated fibroblasts in human breast cancer conditions. Based on previous studies, the NLRP3 inflammasome plays a key role in cancer metastasis and is considered a key pathway for cancer therapy.

Euphorbia L. are traditional medicine used in folk medicine practice (23). The seeds of *Euphorbia lathyris L*., a plant of the *Euphorbiaceae* family, are traditional Chinese medicinal materials in China. They have various biological activities, including anti-inflammatory, antiviral and antitumor activities, and have been used to treat diseases such as edema, ascites and cancer (24). The active ingredients extracted from their seeds can be divided into 21 species, which are Euphorbia factor L1-L21 (EFL1-21). Among them, Euphorbia factor L2 (EFL2) has attracted increasing attention in recent years because of its anticancer effect. For instance, Lin *et al* (24) confirmed that EFL2 promoted the apoptosis process of lung cancer cells A549 through mitochondrial channels. Fan *et al* (25) demonstrated that EFL2 inhibited tumor growth by inhibiting the proliferation and migration of SMMC-7721 and Hep G2 cells through STAT3 phosphorylation. In addition, EFL2 has anti-inflammatory effects; Zhang *et al* (26) reported that it can reduce lipopolysaccharide-induced inflammation in mice by inhibiting NF-κB activation. However, whether EFL2 exerts an inhibitory effect on breast cancer metastasis remains unclear.

Based on the anticancer and anti-inflammatory effects of EFL2, and the critical role of the NLRP3 inflammasome in cancer metastasis, it was investigated whether EFL2 could exert an inhibitory effect on breast cancer metastasis through the inflammasome NLRP3. Therefore, the present study attempted to explore whether EFL2 could inhibit the generation of breast cancer ascites by constructing a mouse breast cancer liver metastasis model, and to further explore whether this inhibition was achieved by inhibiting the activation of the NLPR3 inflammasome.

Materials and methods

Chemicals and antibodies. Antibodies against NLRP3 (cat. no. 13158), IL-1β (cat. no. 12703), caspase 1 (cat. no. 24232), cleaved-caspase1 (cat. no. 89332), GAPDH (cat. no. 5174), and Goat Anti-Rabbit IgG (H+L) HRP (cat. no. 14708) were purchased from Cell Signaling Technology, Inc. Antibodies specifically against CD4 (cat. no. Ab183685) and CD8 (cat. no. Ab209775) were purchased from Abcam. Dulbecco's modified Eagle medium (DMEM) and fetal bovine serum (FBS) were purchased from Sigma-Aldrich; Merck KGaA. Dimethyl sulfoxide (DMSO), trypsin, penicillin-streptomycin solution, multicolor protein marker, Tween 20 and sodium dodecyl sulfate-polyacrylamide gel electrophoresis (SDS-PAGE) were purchased from Beijing Solarbio Science & Technology Co., Ltd. Polyvinylidene fluoride membranes (PVDF) were purchased from MilliporeSigma and the ECL reagent was purchased from COWIN Biotech Co., Ltd. BSA was obtained from Shanghai Aladdin Biochemical Technology Co., Ltd. HiScript II Q RT SuperMix for qPCR, Taq MasterMix and AceQ qPCR SYBR Green Master Mix were purchased from Vazyme Biotech, Cho., Ltd.

Animals. A total of 81 female BALB/c mice (27), 4-6 weeks old, weighing 15-18 g were purchased from the Laboratory Animal Center of Nanjing University of Chinese Medicine. Mice were kept at 22±2˚C with a 12/12-h light/dark cycle and given free access to water and food. Euthanasia of mice was performed using cervical dislocation and subsequently tissues were obtained from mice. All animal procedures were approved by the Institutional Animal Care and Use Committee of Nanjing University of Chinese Medicine (approval no. 202205A137; Nanjing, China) and conducted in accordance with the Guidelines of Accommodation and Care for Animals formulated by the Chinese Convention for the Protection of Vertebrate Animals Used for Experimental and Other Scientific Purposes. The minimum number of animals required to obtain consistent data was used. The humane end point of animal studies was selected for euthanasia when the animal has lost >20% of its body weight during the experiment or was too weak to perform or not tolerating pain, or the mean maximum diameter of the mouse tumor was ≥2 cm. None of the humane endpoints considered was encountered in the course of the current study.

Cell culture. 4T1 cells were obtained from the Shanghai Institute of Biochemistry and Cell Biology. Cells were cultured in DMEM supplemented with 10% FBS, 2 mM L-glutamine and 2% penicillin/streptomycin. Cells were cultured at 37˚C in a humidified atmosphere with 5% CO_2.

Study design

Construction of a breast cancer liver metastasis model. A total of 200 μl of wild or NLRP3 overexpressed 4T1 cells (resuspended in PBS) with a concentration of $2.5x10^7$/ml was injected subcutaneously into the back of the scapula of female BALB/c mice to establish a subcutaneous tumor model of 4T1 cells in female BALB/c mice. The tumor volume of the mice inoculated with cancer cells was measured every 3 days after modeling. When the diameter of the tumor was ≥1 cm, the tumor was removed, and the tumor was cut into a size of 1 mm^3, and then placed in Matrigel in an ice bath.

Female BALB/c mice were anesthetized with 50 mg/kg sodium pentobarbital. The left lobe of the liver was exposed by laparotomy, and the blind cavity was punctured in the left lobe of the liver with a 25G syringe needle, then pressed to stop bleeding and remove blood residue. The tumor mass adhered with Matrigel was placed in the blind end duct on the liver and sutured, and the wound was disinfected with active iodine. The mice were placed on a heating pad and fed a normal diet after waking up. The weight of the mice was measured every week, and the abdominal circumference of the mice was recorded. The drug intervention began 10 days after the operation and was administered for a total of 2 weeks. All mice were sacrificed on the second day of the last administration. The volume of ascites, tumor volume and weight of mice were recorded (28).

Grouping and drug treatments in mice

i) Normal model. The mice were randomly divided into 5 groups, 9 mice in each group, which were normal mice control group, model group, EFL2 low-dose group (25 mg/kg/day), EFL2 high-dose group (50 mg/kg/day) and positive Drug doxorubicin group (5 mg/kg/day) (29). EFL2 was intragastrically administered once a day, and the positive drug was intraperitoneally injected once every 3 days. A total of 2 weeks was the duration of administration, and all mice were sacrificed the day after the last administration.

ii) NLRP3 overexpression model. Firstly, the 4T1 cell line with NLRP3 overexpression [puromycin (10 μg/ml) was used for selection] was constructed; the NLRP3 overexpression lentivirus was provided by Nanjing Bivoli Medical Research Institute Co., Ltd. The lentivirus titer was $1.0x10^8$ TU/ml, the transfection MOI value was 20, and the transfection time was 12-24 h. Then the model was established as aforementioned. The mice were randomly divided into 4 groups with 9 mice in each group, namely model group (WT 4T1 cells), WT 4T1 cells + EFL2 high-dose group (50 mg/kg/day), NLRP3 overexpression 4T1 cells group, and NLRP3 overexpression 4T1 cells + EFL2 high dose group (50 mg/kg/day). The mice were intragastrically administered once a day for a total of 2 weeks, and all mice were sacrificed on the second day of the last administration.

Immunohistochemistry. The tumor tissues fixed for 24 h at 4˚C in 4% paraformaldehyde were dehydrated and embedded in paraffin, and the tissues were cut into 4-μm sections by using a rotary microtome. Sections were dewaxed and rehydrated with xylene and graded ethanol in turn. Antigen retrieval was performed using sodium citrate antigen retrieval solution for 10 min, and then incubated with 3% hydrogen peroxide at room temperature for 10 min. After blocking with 5% goat serum (Beyotime Institute of Biotechnology) blocking solution for 30 min, the primary antibodies (rabbit anti-CD4:1:1,000; rabbit anti-CD8:1:2,000) were incubated at 4˚C overnight. The primary antibody was discarded the next day, and the HRP-labeled Goat Anti-Rabbit IgG (H+L) secondary antibody (1:1,000) was incubated at room temperature for 1 h. Then the freshly prepared DAB chromogenic solution was used to develop color for 1-20 min, and the color development was observed under the light microscope. Sections were immersed in hematoxylin staining solution for 4 min and washed in tap water for 2 min. Then the acid differentiation solution was used to differentiate for 15 sec, and the blue was reversed under running water for 20 min. The sections were dehydrated with graded ethanol, rendered transparent with xylene, and mounted with neutral gum. Finally, a light microscope was used for microscopic examination, and image acquisition and analysis were performed.

Hematoxylin and eosin staining. The tumor, liver and small intestine tissues fixed for 24 h at 4˚C in 4% paraformaldehyde were dehydrated and embedded in paraffin, and then the paraffin block was cut into 4-μm sections using a rotary microtome. Sections were successively dewaxed with xylene, dehydrated with different concentrations of ethanol, stained with hematoxylin nucleus, differentiated by differentiation medium, stained with eosin cytoplasm, dehydrated with different concentrations of ethanol, cleared with xylene, and mounted with neutral resin. The tissue sections were observed under a light microscope.

Western blot analysis. Total protein from tumor tissues *in vivo* was extracted using RIPA cell lysis buffer (Beyotime Institute of Biotechnology) supplemented with PMSF, protease inhibitors and phosphatase inhibitors. The protein concentration was determined using the BCA protein quantification kit according to the manufacturer's instructions. Equal amounts of protein samples (40 μg) were loaded and separated in 10% SDS-PAGE. After transferring to the PVDF membrane, membranes were blocked with 5% BSA at room temperature for 1 h and incubated with the following primary antibodies: NLRP3 (1:1,000), IL-1β (1:1,000), caspase 1 (1:1,000) and cleaved-caspase1 (1:1,000) overnight at 4˚C, followed by incubation with the HRP-labeled Goat Anti-Rabbit IgG (H+L) secondary antibody (1:3,000) at room temperature for 1 h. Finally, the visualization of the membranes was performed using enhanced chemiluminescence (ECL reagent; COWIN Biotech Co., Ltd.). The membranes were then visualized using an imaging system (Bio-Rad Laboratories, Inc.) and quantified using the ImageJ 1.8.0 software (National Institutes of Health).

Immunofluorescence. Tumor tissue (4% paraformaldehyde-fixed) was dehydrated and embedded in paraffin, followed by sectioning, deparaffinization, hydration, antigen retrieval and blocking (as aforementioned in the

'Immunohistochemistry' paragraph), followed by an overnight primary antibody (NLRP3; 1:500; cat. no. PA5-79740; Thermo Fisher Scientific, Inc.) incubation at 4˚C. After washing 3 times with PBS, sections were incubated with FITC-conjugated secondary antibody (1:1,000; cat. no. ab150077; Abcam) for 1 h at 37˚C. Next, the slices were washed and mounted in a fade-resistant mounting medium with DAPI (5 μg/ml). Finally, the sections were evaluated on a fluorescence microscope.

Reverse transcription-quantitative PCR (RT-qPCR). Total RNA from mice tumor tissues (10-50 mg) was prepared by using TRIzol reagent (Vazyme Biotech Co., Ltd). cDNA was generated by HiScript II Q RT SuperMix for qPCR Kit according to the manufacturer's instructions. qPCR was performed using AceQ qPCR SYBR Green Master Mix. The qPCR thermal cycling conditions were as follows: An initial denaturation step at 95˚C for 5 min, followed by 40 cycles of denaturation at 95˚C for 10 sec and annealing/extension at 60˚C for 30 sec. Each sample was subjected to PCR amplification in triplicate. Data were analyzed with $2^{-\Delta\Delta Cq}$ method (30), using GAPDH for normalization. The mRNA levels of NLRP3, IL-1β and GAPDH in tumor tissues were accessed. The sequences of the primers used are shown in Table I.

MTT assay. MTT assay was used to detect the effect of different treatments on cell viability. Briefly, 4T1 cells were cultured for 24 h in 96-well plates at a density of 8,000 cells/well. The cells were treated with different concentrations of drug-containing serum 24 h after the cell model was prepared *in vitro*. After 24 h of treatment, 20 μl MTT (5 mg/ml) was added to each well, and the supernatant was discarded for 4 h. After that, 150 μl DMSO was added to each well, and the dirty crystals were fully dissolved using low-speed oscillations for 10 min. Finally, OD values were determined by using an enzymic labelled meter at 570 nm wavelength.

EdU cell proliferation assay. 4T1 cells and EFL2-treated 4T1 cells were incubated into 96-well culture plates at a density of $2x10^3$ cells/well and incubated for 24 h. The EdU analysis kit (cat. no. C6015S; US Everbright Inc.) was used to analyze and evaluate cell proliferation, and the specific method was carried out following the instructions provided by the manufacturer. The samples were analysed with a fluorescence microscope.

Statistical analysis. GraphPad Prism 7.0 software (Dotmatics) was used for all statistical analyses. The mean ± SD was used to represent the results. Data were analyzed using one-way analysis of variance (ANOVA) with Dunnett's multiple comparisons test or Tukey's multiple comparisons test. $P<0.05$ and $P<0.01$ were considered to indicate a significant and very significant difference, respectively.

Results

Effects of EFL2 on ascites generation in breast cancer liver metastasis. To investigate the effects of EFL2 on generation of ascites in liver metastasis model of breast cancer, the abdominal circumference, the volume of peritoneal fluid and body weight in mice, as well as liver tumor volume and weight, were measured. Images of the mice and tumors were captured (Fig. 1A) and compared with the control group; the abdominal circumference and ascites' volume of the mice in the model group were significantly increased, but they were significantly decreased after EFL2 and positive drug treatment (Fig. 1B and C). The body weight, liver tumor volume and weight of the mice were then measured between the two time periods. The weight of mice in the control group was not significantly different from that in the model group, but the weight of the mice in the administration group was significantly lower than that in the model group (Fig. 1D). The tumor volume and weight in the liver of mice in the model group were considerably smaller than those in the administration group, and the difference was most significant with the positive drug group (Fig. 1E and F). These results suggested that EFL2 could inhibit the generation of ascites in liver metastasis model of breast cancer. However, because the tumor-bearing mice tended anorexia, the diet decreased, thus the weight of the administration group was reduced. The tumor volume and weight in the liver of the mice in the model group were the smallest, and the trend was opposite to that of the ascites volume, which might be due to ascites caused by metastasis of a large number of solid tumors in the model group, and the migration amount decreased in each administration group.

Table I. Primers for reverse transcription-quantitative PCR.

Gene name	Primer sequence (5'→3')
NLR family pyrin domain containing-3	F: TCCACAATTCTGACCCACAA
	R: ACCTCACAGAGGGTCACCAC
IL-1β	F: TTGACGGACCCCAAAAGATG
	R: AGGACAGCCCAGGTCAAAG
GAPDH	F: GCCTCCTCCAATTCAACCCT
	R: CTCGTGGTTCACACCCATCA

F, forward; R, reverse.

EFL2 inhibits liver inflammation and tumor migration in breast cancer liver metastasis. To investigate the effect of EFL2 on liver tumors, liver and small intestine tissues as well as liver tumors were examined using H&E staining. The results of H&E staining of liver tissue revealed that there were inflammatory cells (the yellow dotted line circles the symbolic inflammatory cell mass) infiltration in the liver tissue of tumor-bearing mice, and the model group had the most, and each administration group attenuated the infiltration of inflammatory cells to varying degrees (Fig. 2A and D). The H&E staining results of the small intestine tissue demonstrated that the small intestine adventitia of the tumor-bearing mice had tumor tissues of different sizes (black arrows), the model group had the largest tumor tissue, and each administration group reduced the migration of tumor cells to the small intestine to varying degrees (Fig. 2B). The results of H&E staining of tumor tissue showed that the arrangement of tumor cells in each administration group was more scattered than that in the model group (Fig. 2C). These results suggested that inhibition of tumor metastasis by EFL2 may be associated with reduced tissue inflammation.

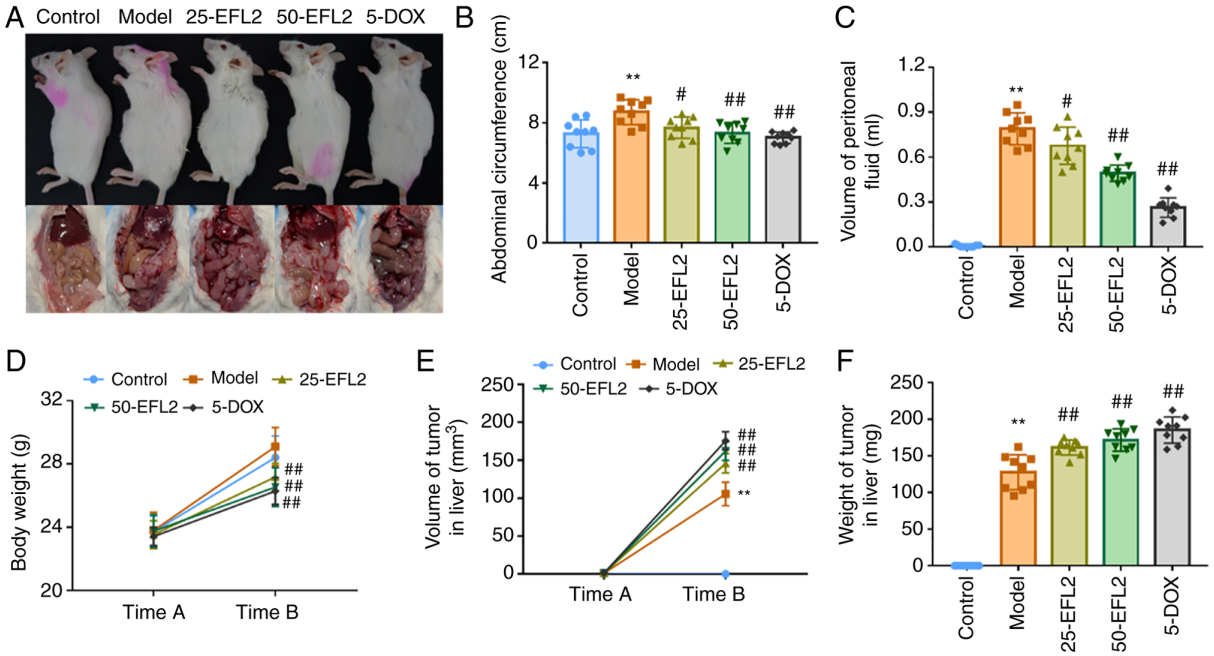

Figure 1. Effects of EFL2 on generation of ascites in breast cancer liver metastasis. (A) Gross appearance and tumor, (B) abdominal circumference, (C) volume of peritoneal fluid, (D) body weight, (E) volume of tumor in the liver and (F) weight of tumor in the liver of Control, Model, Low-dose EFL2 (25-EFL2) treatment, High-dose EFL2 (50-EFL2) treatment and Positive drug (5-DOX) treatment (n=9). Mean ± SD as data representation. **P<0.01 vs. the control; $^{\#}$P<0.05 and $^{\#\#}$P<0.01 vs. the model. EFL2, Euphorbia factor L2; DOX, doxorubicin.

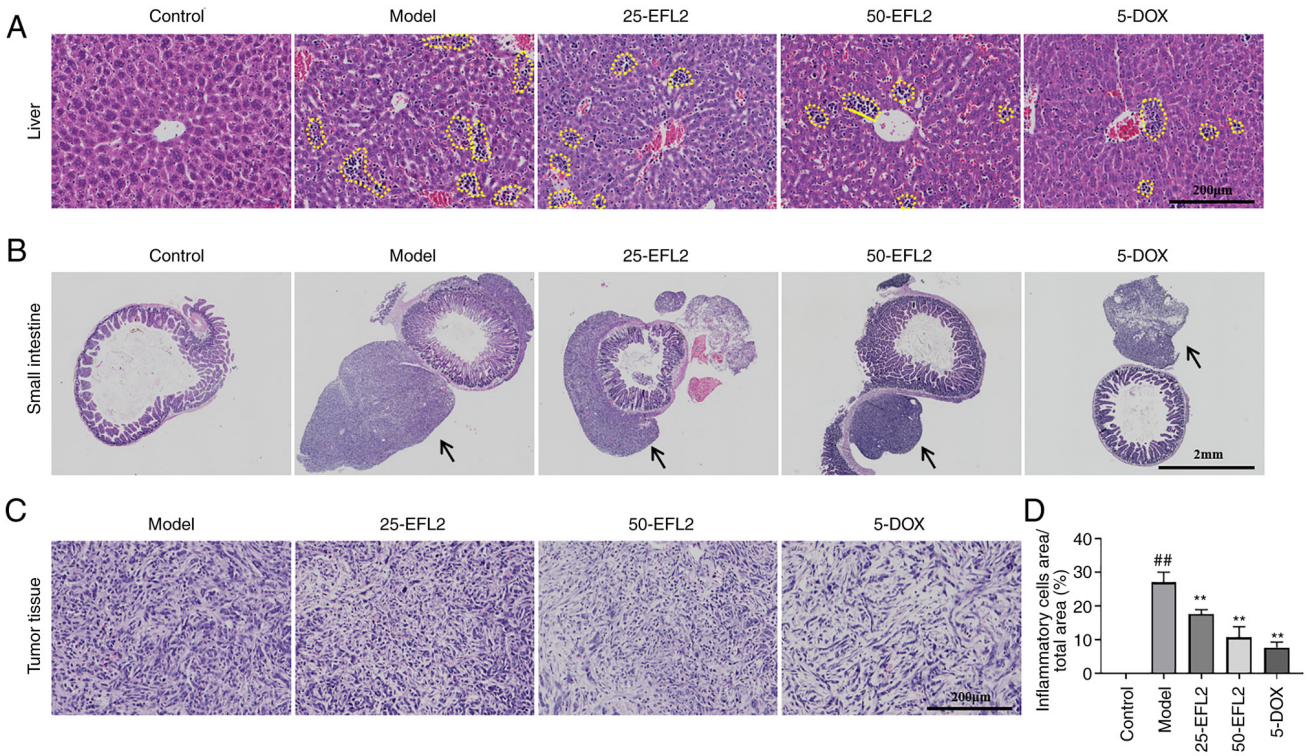

Figure 2. EFL2 inhibits liver inflammation and tumor migration in breast cancer liver metastasis. H&E staining of (A) liver tissues (Scale bars, 200 μm), (B) small intestine tissues (Scale bars, 2 mm), and (C) tumor tissues (Scale bars, 200 μm) of Control, Model, Low-dose EFL2 (25-EFL2) treatment, High-dose EFL2 (50-EFL2) treatment, Positive drug (5-DOX) treatment. (D) Quantitative analysis of the yellow dotted circle in Fig. 2A (expressed as a percentage of the total area of the yellow dotted circle) (n=3). Mean ± SD as data representation. $^{\#\#}$P<0.01 vs. the control and **P<0.01 vs. the model. The yellow dotted circles in Fig. 2A represent symbolic inflammatory cell masses in liver tissue. The black arrows in Fig. 2B indicate tumor tissue of different sizes in the outer small intestine of tumor-bearing mice. EFL2, Euphorbia factor L2; DOX, doxorubicin.

EFL2 inhibits tumor metastasis by inhibiting NLRP3 in breast cancer liver metastasis. NLRP3 is the most studied and best characterized type of inflammasome (16). The aforementioned findings of the present study suggested that the inhibition of

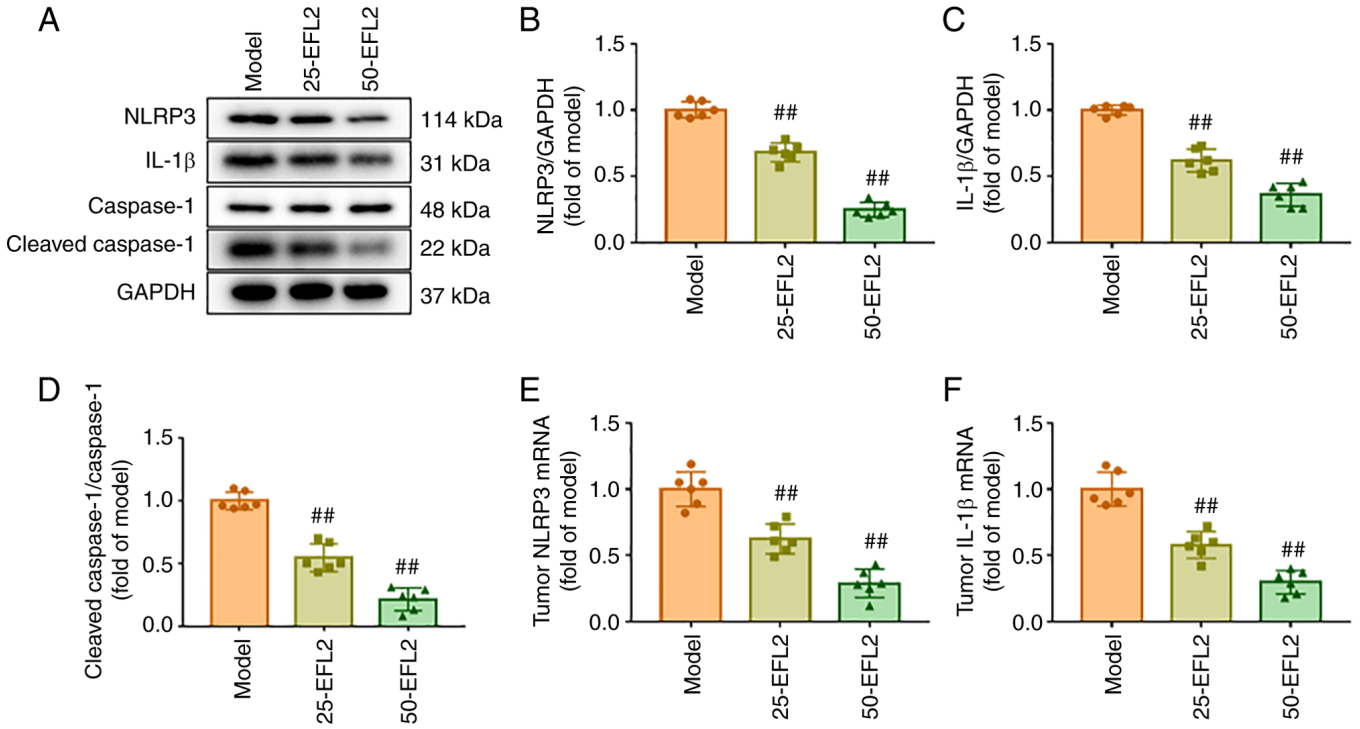

Figure 3. EFL2 inhibits tumor metastasis by inhibiting NLRP3 in breast cancer liver metastasis. (A) The expression levels of NLRP3, cleaved-caspase1, caspase1 and IL-1β in tumor tissues of Model, Low-dose EFL2 (25-EFL2) treatment and High-dose EFL2 (50-EFL2) treatment were detected by western blotting. (B and C) Normalized and quantified NLRP3 and IL-1β expression levels to GAPDH. (D) Normalized and quantified cleaved-caspase1 expression level to caspase1 (n=6). (E and F) The mRNA transcription of NLRP3 and IL-1β in tumor tissues of Model, Low-dose EFL2 (25-EFL2) treatment and High-dose EFL2 (50-EFL2) treatment were detected by reverse transcription-quantitative PCR (n=6). Mean ± SD as data representation. $^{\#\#}$P<0.01 vs. the model. EFL2, Euphorbia factor L2; NLRP3, NLR family pyrin domain containing-3.

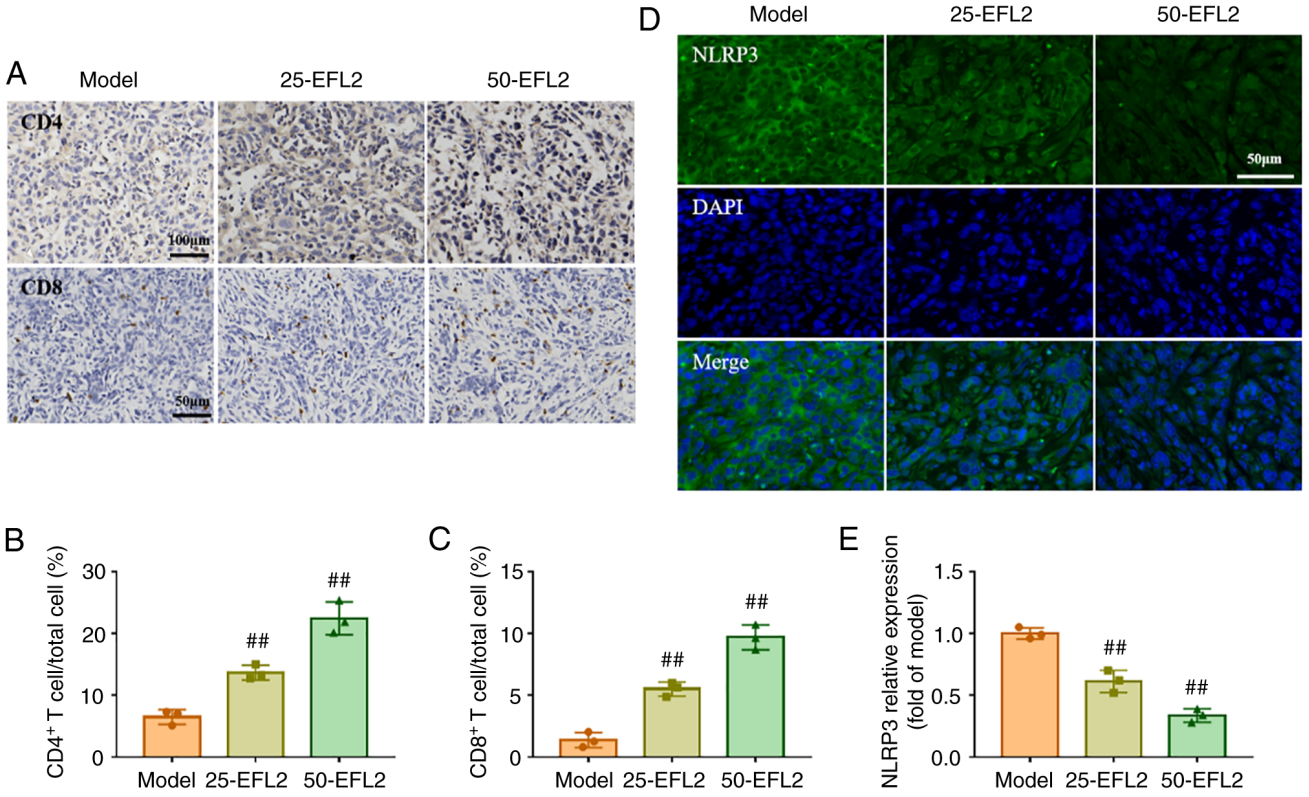

Figure 4. EFL2 enhances immune cell infiltration in the tumor. (A) The $CD4^+$ (Scale bars, 100 μm) and $CD8^+$ (Scale bars, 50 μm) T cells in tumor tissues of the Model, Low-dose EFL2 treatment (25-EFL2) and High-dose EFL2 (50-EFL2) treatment were measured by immunohistochemistry. (B and C) Quantifications of immunohistochemistry (n=3 in each group). (D) The expression of NLRP3 in tumor tissues of Model, Low-dose EFL2 (25-EFL2) treatment and High-dose EFL2 (50-EFL2) treatment were analyzed by immunofluorescent staining. (E) Quantifications of immunofluorescence staining (n=3 in each group). Scale bar, 50 μm. Mean ± SD as data representation. $^{\#\#}$P<0.01 vs. the model. EFL2, Euphorbia factor L2; NLRP3, NLR family pyrin domain containing-3.

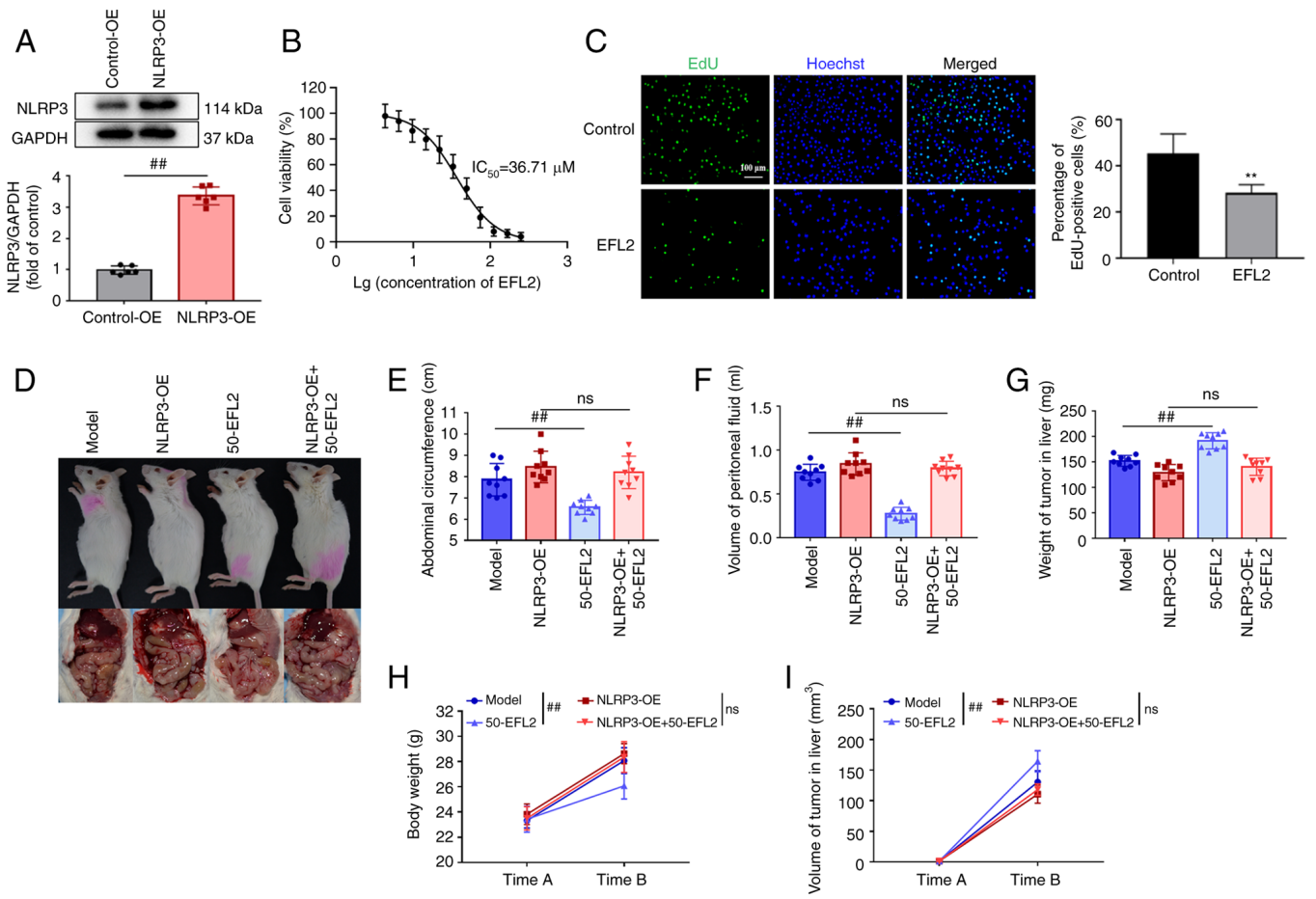

Figure 5. EFL2 reduces generation of ascites in breast cancer liver metastasis by inhibiting NLRP3 activation. (A) Analysis of NLRP3 expression in the control group and NLRP3 overexpression group of 4T1 cells using western blotting and quantitative analysis of the NLRP3 expression level to GAPDH (n=6). (B) The effects of different concentrations of EFL2 on the viability of 4T1 cells were detected by MTT assay (n=6). (C) Edu cell proliferation assay was used to detect the effect of 36.71 μm EFL2 on the proliferation of 4T1 cells (Scale bars, 50 μm; n=6), **P<0.01 vs. the control. (D) Gross appearance and tumor, (E) abdominal circumference, (F) volume of peritoneal fluid, (G) weight of tumor in the liver, (H) body weight and (I) volume of tumor in the liver of Model, NLRP3 overexpression (NLRP3-OE), High-dose EFL2 treatment (50-EFL2) and NLRP3 overexpression plus High-dose EFL2 treatment (NLRP3-OE+50-EFL2) (n=9). Mean ± SD as data representation. $^{\#\#}$P<0.01 vs. the model. EFL2, Euphorbia factor L2; NLRP3, NLR family pyrin domain containing-3; OE, overexpression; ns not significant.

tumor metastasis by EFL2 may be related to the reduction of tissue inflammation, and that the reduction of inflammation may be related to NLRP3. To investigate this hypothesis, the protein expression levels of NLRP3, cleaved-caspase1, total caspase1 and IL-1β in tumor tissues were detected using western blotting, and the mRNA transcription of NLRP3 and IL-1β in tumor tissues were identified using RT-qPCR. The results of western blotting revealed that compared with the model group, the expression levels of NLRP3, cleaved-caspase1/caspase1 and IL-1β in tumor tissues were significantly decreased after EFL2 treatment, and the effect of high concentration of EFL2 was more obvious (Fig. 3A-D). The results of RT-qPCR were consistent with those of western blotting (Fig. 3E and F). These results suggested that NLRP3 was involved in the inhibitory effect of EFL2 on tumor metastasis and tissue inflammation.

EFL2 enhances immune cell infiltration in the tumor. The proportion of CD4 and CD8 cells in tumor tissue was further detected by immunohistochemistry, and the expression of NLRP3 was detected by immunofluorescence. The immunohistochemical results demonstrated that compared with the model group, the CD4 and CD8 T cells in the tumor tissue after EFL2 treatment was greatly increased, and the high concentration of EFL2 was more significant (Fig. 4A-C). The immunofluorescence results revealed strong linear staining of NLRP3 and nuclei in the model group. This situation was weak and discontinuous in EFL2-treated groups. In addition, the expression level of NLRP3 was significantly decreased in EFL2-treated groups compared with the model group (Fig. 4D and E). In conclusion, EFL2 inhibited NLRP3 expression and enhanced immune cell infiltration in tumor tissues, reduced inflammation, and in turn inhibited tumor cell metastasis.

EFL2 reduces ascites generation in breast cancer liver metastasis by inhibiting NLRP3 inflammasome activation. To further verify whether EFL2 inhibits tumor metastasis by inhibiting the activation of NLRP3, gene overexpression was used. First, the NLRP3-overexpressing 4T1 cell line was constructed, followed by tumor seeding. Validation of overexpression by western blotting, and overexpression of NLRP3 was effective (Fig. 5A). In addition, the effect of EFL2 on 4T1 cells was examined *in vitro* by MTT assay and Edu

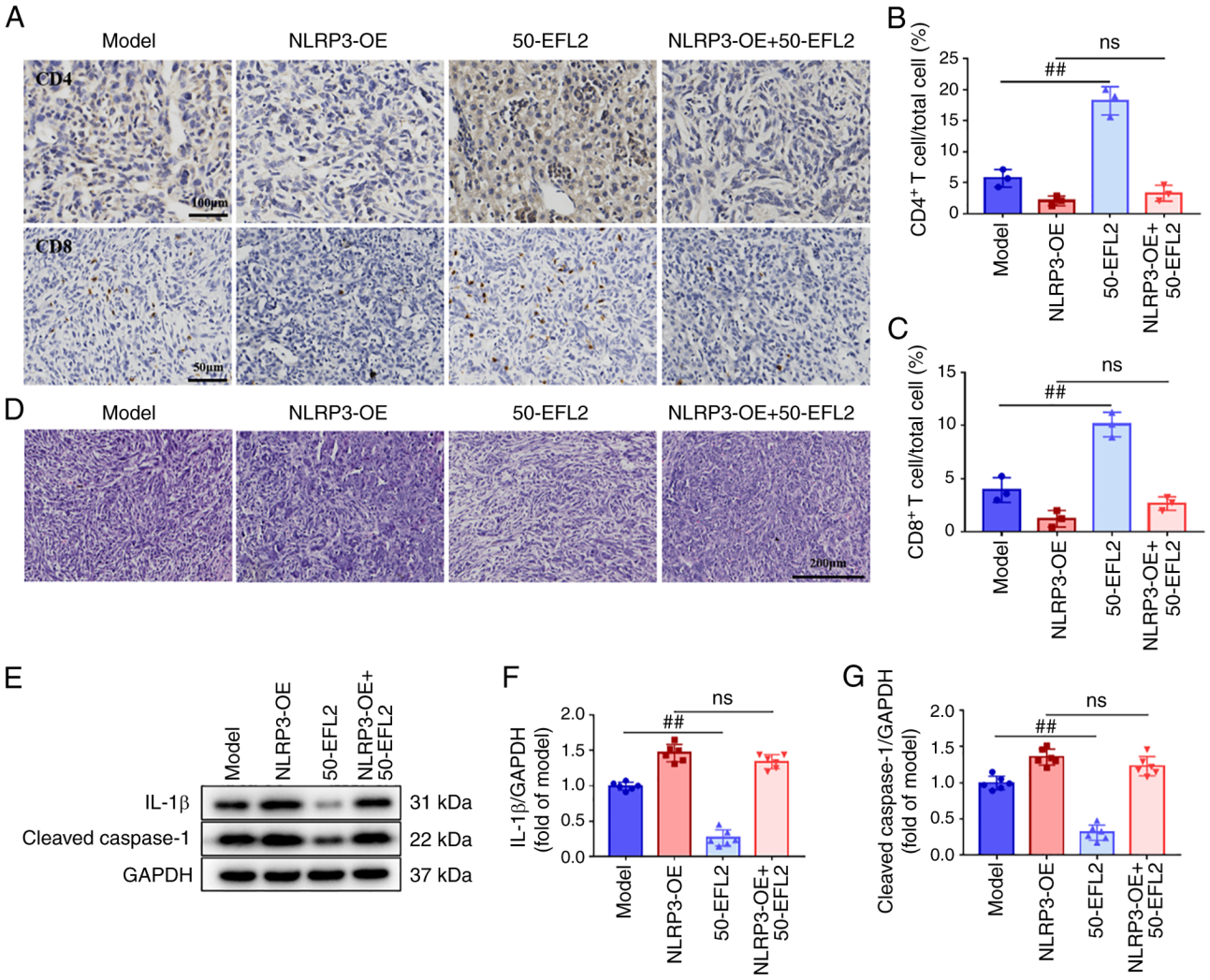

Figure 6. EFL2 inhibits tumor metastasis via inhibiting NLRP3 activation. (A) The CD4 (Scale bars, 100 μm) and CD8 (Scale bars, 50 μm) T cells in tumor tissues of Model, NLRP3 overexpression (NLRP3-OE), High-dose EFL2 treatment (50-EFL2) and NLRP3 overexpression plus High-dose EFL2 treatment (NLRP3-OE+50-EFL2) were measured by immunohistochemistry. (B and C) Quantifications of immunohistochemistry (n=3). (D) H&E staining of tumor tissues (Scale bars, 200 μm) of Model, NLRP3 overexpression (NLRP3-OE), High-dose EFL2 treatment (50-EFL2) and NLRP3 overexpression plus High-dose EFL2 treatment (NLRP3-OE+50-EFL2). (E) The expression levels of NLRP3 and cleaved-caspase1 in tumor tissues of Model, NLRP3 overexpression (NLRP3-OE), High-dose EFL2 treatment (50-EFL2) and NLRP3 overexpression plus High-dose EFL2 treatment (NLRP3-OE+50-EFL2) were detected by western blotting. (F and G) Normalized and quantified protein levels to GAPDH (n=6). Mean ± SD as data representation. $^{\#\#}$P<0.01 vs. the model. EFL2, Euphorbia factor L2; NLRP3, NLR family pyrin domain containing-3; OE, overexpression; ns not significant.

experiment. The results of the MTT assay identified that the IC_{50} of EFL2 on 4T1 cells was 36.71 μm (Fig. 5B), and further Edu assay revealed that this concentration of EFL2 could inhibit the proliferation of 4T1 cells (Fig. 5C). Images of the mice and tumors were captured (Fig. 5D), and to investigate whether EFL2 reduced generation of ascites in liver metastasis model of breast cancer by inhibiting NLRP3 inflammasome activation, the abdominal circumference, ascites volume, and body weight of the mice, as well as liver tumor volume and weight, were measured. Compared with the model group, the abdominal circumference, volume of peritoneal fluid and body weight of the EFL2 treatment group were significantly decreased, but there was no significant difference between the NLRP3 overexpression group and the NLRP3 overexpression plus EFL2 treatment group (Fig. 5E, F and H). By contrast, compared with the model group, the liver tumor weight and tumor volume in the EFL2-treated group were significantly increased, but there was no significant difference between the NLRP3 overexpression group and the NLRP3 overexpression plus EFL2 treatment group (Fig. 5G and I). These results further demonstrated that EFL2 inhibits ascites' generation in liver metastasis model of breast cancer by inhibiting the activation of NLRP3.

EFL2 inhibits tumor metastasis via inhibiting NLRP3 activation. The aforementioned experiments proved that EFL2 inhibits the formation of ascites by inhibiting the activation of NLRP3, but the specific mechanism remains unclear. Therefore, in order to observe the effect of overexpression of NLRP3 on the mechanism, liver tumors were detected using immunohistochemistry and H&E staining, and the expression levels of cleaved-caspase1 and IL-1β in tumor tissues were detected by western blotting. Immunohistochemical results demonstrated that compared with the model group, the levels of CD4 and CD8 T cells in the EFL2-treated group were significantly increased, while there was no significant difference between the

NLRP3 overexpression group and the NLRP3 overexpression plus EFL2 treatment group (Fig. 6A-C). The results of H&E staining revealed that the tumor cells in the EFL2-treated group were scattered compared with the model group, and there was no significant difference between the NLRP3 overexpression group and the NLRP3 overexpression plus EFL2 treatment group (Fig. 6D). In addition, western blotting results identified that compared with the model group, the expression levels of cleaved-caspase1 and IL-1β in the EFL2-treated group were significantly decreased, while there was no significant difference between the NLRP3 overexpression group and the NLRP3 overexpression plus EFL2 treatment group (Fig. 6E-G). These results suggested that EFL2 enhances immune cell infiltration and suppresses tumor cell metastasis by inhibiting NLRP3 activation, which may be the mechanism by which EFL2 inhibits generation of ascites in breast cancer liver metastasis.

Discussion

Breast cancer is a complex disease that has been found to be the second leading cause of cancer-related death in women. Although there are numerous effective treatments, the mortality rate due to breast cancer metastasis is gradually increasing (31). Nearly all deaths from breast tumors can be attributed to distant metastasis. Metastasis is the leading cause of death in the vast majority of patients with breast cancer. Most drugs treat breast cancer metastases poorly, highlighting the urgent need to discover new drug treatments (32).

Compelling evidence confirms that inflammation plays an important role in tumor metastasis (33-35). Lunasin attenuates obesity-associated 4T1 breast cancer cell metastasis through anti-inflammatory properties, as previously demonstrated (36). In addition, studies have shown that inflammation is associated with immune response evasion and poor prognosis in cancer (37,38). Based on the close link between inflammation and cancer metastasis and the effect of inflammation on poor cancer prognosis, it was aimed to determine whether EFL2 has an effect on ascites in liver metastases from breast cancer. By constructing a breast cancer liver metastasis model, it was found that compared with the model group, the production of ascites after EFL2 treatment was significantly reduced, indicating that EFL2 can effectively inhibit the production of ascites in the breast cancer liver metastasis model. However, the weight of the mice in the control group was larger than that of the administration groups and there was no significant difference with the model group, which may be due to the tendency of anorexia in the tumor-bearing mice to reduce their diet and body weight. In addition, the tumor volume and weight in the liver of the mice in the model group were smaller than those in the administration group, which was the opposite of the ascites' volume. This may be due to a large number of solid tumor metastases in the liver of the model group and the decrease of metastases in each administration group. Detection of the liver, small intestine and tumor tissue by H&E staining demonstrated that EFL2 attenuated inflammatory cell infiltration and tumor cell migration.

To date, numerous studies have shown that activation of inflammatory signaling pathways is critical for cancer development and metastasis (39). For example, the IL-6/JAK/STAT3 pathway is abnormally overactivated in numerous types of cancer, and this overactivation is often associated with poor clinical prognosis (40). Liang *et al* (41) confirmed that cancer-derived exosome TRIM59 promotes lung cancer progression by regulating macrophage NLRP3 inflammasome activation. It has been reported that inflammasomes are aberrantly expressed and activated in a variety of malignancies and play an important role in tumor development (42). Among them, NLRP3, as the most studied and best characterized inflammasome type, plays an important role in cancer metastasis. Shao *et al* (43) reported that NLRP3 can promote the metastasis of colorectal cancer cells by regulating epithelial-mesenchymal transition. Moreover, it has been previously revealed that the NLRP3 inflammasome in macrophages drives colorectal cancer metastasis to the liver (44). In addition, it has been identified that inhibition of the NLRP3 inflammasome in the tumor microenvironment inhibits the metastatic potential of cancer cells (45). Therefore, in the present study, the mRNA transcription and protein expression levels of NLRP3 and related molecules were investigated in tumor tissues, and the proportions of CD4 and CD8 T cells were examined. It was found that the mRNA transcription and protein expression levels of NLRP3 and its related molecules were significantly decreased in a dose-dependent manner by EFL2 treatment. Furthermore, it was demonstrated that EFL2 led to an increase in CD4 and CD8 T cells and enhanced immune cell infiltration. Next, *in vivo* overexpression experiments of NLRP3 showed that overexpression of NLRP3 significantly attenuated the inhibitory effect of EFL2, suggesting that these beneficial effects of EFL2 may be related to the downregulation of NLRP3 signaling.

In conclusion, the current experimental data suggested that EFL2 has a significant inhibitory effect on ascites of breast cancer liver metastasis *in vivo*, possibly by inhibiting tumor cell metastasis by downregulating the expression of NLRP3. Therefore, the application of EFL2 in combination with current conventional adjuvant therapy may provide a new therapeutic strategy for breast cancer patients with liver metastases. However, further studies are needed to confirm the present results and evaluate the role of EFL2 in breast cancer liver metastasis.

In summary, it was demonstrated in the present study that EFL2 had a significant inhibitory effect on ascites of breast cancer liver metastasis *in vivo*, possibly inhibiting tumor cell metastasis by downregulating NLRP3 expression. These findings suggested that the natural drug EFL2 may be an effective drug treatment option for breast cancer liver metastasis. However, the mechanism of action of EFL2 on tumor cells *in vitro* was not explored; and the *in vivo* study was not particularly in-depth. In future studies, this question shall be further investigated by the authors.

Acknowledgements

Not applicable.

Funding

The present study was supported by the Natural Science Foundation of the Higher Education Institutions of Jiangsu (grant no. 20KJB360013), the Science and Technology Support

Project of Suzhou (grant no. SYS2020080) and Suzhou Basic Research Program (grant no. SKY2023042).

Availability of data and materials

The datasets used and/or analyzed during the current study are available from the corresponding author on reasonable request.

Authors' contributions

DJ performed investigation and data curation. XL developed methodology. RT wrote the original draft of the manuscript and contributed to the acquisition of data. YZ curated data. LZ acquired funding and contributed to the conception or design of the study. All authors read and approved the final version of the manuscript. DJ and LZ confirm the authenticity of all the raw data.

Ethics approval and consent to participate

The animal study protocol was approved (approval no. 202205A037) by Nanjing University of Chinese Medicine Laboratory Animal Center (Nanjing, China).

Patient consent for publication

Not applicable.

Competing interests

The authors declare that they have no competing interests.

References

1. Bray F, Ferlay J, Soerjomataram I, Siegel RL, Torre LA and Jemal A: Global cancer statistics 2018: GLOBOCAN estimates of incidence and mortality worldwide for 36 cancers in 185 countries. CA Cancer J Clin 68: 394-424, 2018.
2. DeSantis CE, Ma J, Goding Sauer A, Newman LA and Jemal A: Breast cancer statistics, 2017, racial disparity in mortality by state. CA Cancer J Clin 67: 439-448, 2017.
3. Tao L, Chu L, Wang LI, Moy L, Brammer M, Song C, Green M, Kurian AW, Gomez SL and Clarke CA: Occurrence and outcome of de novo metastatic breast cancer by subtype in a large, diverse population. Cancer Causes Control 27: 1127-1138, 2016.
4. Hazem RM, Mohamed AA, Ghareb N, Mehanna ET, Mesbah NM, Abo-Elmatty DM and Elgawish MS: Anti-cancer activity of two novel heterocyclic compounds through modulation of VEGFR and miR-122 in mice bearing Ehrlich ascites carcinoma. Eur J Pharmacol 892: 173747, 2021.
5. Guo W, Zhang S and Liu S: Establishment of a novel orthotopic model of breast cancer metastasis to the lung. Oncol Rep 33: 2992-2998, 2015.
6. Kipps E, Tan DS and Kaye SB: Meeting the challenge of ascites in ovarian cancer: New avenues for therapy and research. Nat Rev Cancer 13: 273-282, 2013.
7. Sangisetty SL and Miner TJ: Malignant ascites: A review of prognostic factors, pathophysiology and therapeutic measures. World J Gastrointest Surg 4: 87-95, 2012.
8. Mikuła-Pietrasik J, Uruski P, Szubert S, Moszyński R, Szpurek D, Sajdak S, Tykarski A and Książek K: Biochemical composition of malignant ascites determines high aggressiveness of undifferentiated ovarian tumors. Med Oncol 33: 94, 2016.
9. Yin T, Wang G, He S, Shen G, Su C, Zhang Y, Wei X, Ye T, Li L, Yang S, *et al*: Malignant pleural effusion and ascites induce epithelial-mesenchymal transition and cancer stem-like cell properties via the vascular endothelial growth factor (VEGF)/Phosphatidylinositol 3-Kinase (PI3K)/Akt/Mechanistic target of rapamycin (mTOR) pathway. J Biol Chem 291: 26750-26761, 2016.
10. Vargas-Villarreal J, Cruz-Ramos M, Espino-Ojeda A, Gutierrez-Hermosillo H, Díaz De Leon-Gonzalez E, Monsivais-Diaz O, Palacios-Corona R, Martinez-Armenta CA, González-Salazar F, Moreno-Treviño MG and Guzman-De La Garza FJ: Acellular fraction from malignant effusions has cytotoxicity in breast cancer cells. Mol Clin Oncol 14: 106, 2021.
11. Gupta V, Yull F and Khabele D: Bipolar tumor-associated macrophages in ovarian cancer as targets for therapy. Cancers (Basel) 10: 366, 2018.
12. Song XD, Wang YN, Zhang AL and Liu B: Advances in research on the interaction between inflammation and cancer. J Int Med Res 48: 300060519895347, 2020.
13. Shen Y, Guo D, Weng L, Wang S, Ma Z, Yang Y, Wang P, Wang J and Cai Z: Tumor-derived exosomes educate dendritic cells to promote tumor metastasis via HSP72/HSP105-TLR2/TLR4 pathway. Oncoimmunology 6: e1362527, 2017.
14. Holl EK, Frazier V, Landa K, Boczkowski D, Sullenger B and Nair SK: Controlling cancer-induced inflammation with a nucleic acid scavenger prevents lung metastasis in murine models of breast cancer. Mol Ther 29: 1772-1781, 2021.
15. Wellenstein MD, Coffelt SB, Duits DEM, van Miltenburg MH, Slagter M, de Rink I, Henneman L, Kas SM, Prekovic S, Hau CS, *et al*: Loss of p53 triggers WNT-dependent systemic inflammation to drive breast cancer metastasis. Nature 572: 538-542, 2019.
16. Tengesdal IW, Menon DR, Osborne DG, Neff CP, Powers NE, Gamboni F, Mauro AG, D'Alessandro A, Stefanoni D, Henen MA, *et al*: Targeting tumor-derived NLRP3 reduces melanoma progression by limiting MDSCs expansion. Proc Natl Acad Sci USA 118: e2000915118, 2021.
17. Sun R, Gu J, Chang X, Liu F, Liang Y, Yang X, Liang L and Tang D: Metabonomics study on orthotopic transplantion mice model of colon cancer treated with astragalus membranaceus-curcuma wenyujin in different proportions via UPLC-Q-TOF/MS. J Pharm Biomed Anal 193: 113708, 2021.
18. Ratajczak MZ, Bujko K, Cymer M, Thapa A, Adamiak M, Ratajczak J, Abdel-Latif AK and Kucia M: The Nlrp3 inflammasome as a 'rising star' in studies of normal and malignant hematopoiesis. Leukemia 34: 1512-1523, 2020.
19. Zaki MH, Vogel P, Body-Malapel M, Lamkanfi M and Kanneganti TD: IL-18 production downstream of the Nlrp3 inflammasome confers protection against colorectal tumor formation. J Immunology 185: 4912-4920, 2010.
20. Li S, Liang X, Ma L, Shen L, Li T, Zheng L, Sun A, Shang W, Chen C, Zhao W and Jia J: MiR-22 sustains NLRP3 expression and attenuates H. pylori-induced gastric carcinogenesis. Oncogene 37: 884-896, 2018.
21. Guo B, Fu S, Zhang J, Liu B and Li Z: Targeting inflammasome/IL-1 pathways for cancer immunotherapy. Sci Rep 6: 36107, 2016.
22. Ershaid N, Sharon Y, Doron H, Raz Y, Shani O, Cohen N, Monteran L, Leider-Trejo L, Ben-Shmuel A, Yassin M, *et al*: NLRP3 inflammasome in fibroblasts links tissue damage with inflammation in breast cancer progression and metastasis. Nat Commun 10: 4375, 2019.
23. Tang J, Cheng X, Yi S, Zhang Y, Tang Z, Zhong Y, Zhang Q, Pan B and Luo Y: *Euphorbia* factor L2 ameliorates the progression of K/BxN serum-induced arthritis by blocking TLR7 mediated IRAK4/IKKβ/IRF5 and NF-kB signaling pathways. Front Pharmacol 12: 773592, 2021.
24. Lin M, Tang S, Zhang C, Chen H, Huang W, Liu Y and Zhang J: Euphorbia factor L2 induces apoptosis in A549 cells through the mitochondrial pathway. Acta Pharm Sin B 7: 59-64, 2017.
25. Fan L, Zhu H, Tao W, Liu L, Shan X, Zhao M and Sun D: Euphorbia factor L2 inhibits TGF-β-induced cell growth and migration of hepatocellular carcinoma through AKT/STAT3. Phytomedicine 62: 152931, 2019.
26. Zhang Q, Zhu S, Cheng X, Lu C, Tao W, Zhang Y, William BC, Cao X, Yi S, Liu Y, *et al*: Euphorbia factor L2 alleviates lipopolysaccharide-induced acute lung injury and inflammation in mice through the suppression of NF-κB activation. Biochem Pharmacol 155: 444-454, 2018.
27. Tallón de Lara P, Castañón H, Vermeer M, Núñez N, Silina K, Sobottka B, Urdinez J, Cecconi V, Yagita H, Movahedian Attar F, *et al*: CD39+PD-1+CD8+ T cells mediate metastatic dormancy in breast cancer. Nat Commun 12: 769, 2021.
28. Lim HI, Yamamoto J, Han Q, Sun YU, Nishino H, Tashiro Y, Sugisawa N, Tan Y, Choi HJ, Nam SJ, *et al*: Response of triple-negative breast cancer liver metastasis to oral recombinant methioninase in a patient-derived orthotopic xenograft (PDOX) model. In Vivo 34: 3163-3169, 2020.

29. Zhang S, Liu X, Abdulmomen Ali Mohammed S, Li H, Cai W, Guan W, Liu D, Wei Y, Rong D, Fang Y, *et al*: Adaptor SH3BGRL drives autophagy-mediated chemoresistance through promoting PIK3C3 translation and ATG12 stability in breast cancers. Autophagy 18: 1822-1840, 2022.
30. Livak KJ and Schmittgen TD: Analysis of relative gene expression data using real-time quantitative PCR and the 2(-Delta Delta C(T)) method. Methods 25: 402-408, 2001.
31. Nirgude S, Mahadeva R, Koroth J, Kumar S, Kumar KSS, Gopalakrishnan V, S Karki SS and Choudhary B: ST09, a novel curcumin derivative, blocks cell migration by inhibiting matrix metalloproteases in breast cancer cells and inhibits tumor progression in EAC mouse tumor models. Molecules 25: 4499, 2020.
32. Papageorgis P, Ozturk S, Lambert AW, Neophytou CM, Tzatsos A, Wong CK, Thiagalingam S and Constantinou AI: Targeting IL13Ralpha2 activates STAT6-TP63 pathway to suppress breast cancer lung metastasis. Breast Cancer Res 17: 98, 2015.
33. De Simone V, Franzè E, Ronchetti G, Colantoni A, Fantini MC, Di Fusco D, Sica GS, Sileri P, MacDonald TT, Pallone F, *et al*: Th17-type cytokines, IL-6 and TNF-α synergistically activate STAT3 and NF-kB to promote colorectal cancer cell growth. Oncogene 34: 3493-3503, 2015.
34. Mishra DK, Rocha HJ, Miller R and Kim MP: Immune cells inhibit the tumor metastasis in the 4D cellular lung model by reducing the number of live circulating tumor cells. Sci Rep 8: 16569, 2018.
35. Yang C, Wang Z, Li L, Zhang Z, Jin X, Wu P, Sun S, Pan J, Su K, Jia F, *et al*: Aged neutrophils form mitochondria-dependent vital NETs to promote breast cancer lung metastasis. J Immunother Cancer 9: e002875, 2021.
36. Hsieh CC, Wang CH and Huang YS: Lunasin attenuates obesity-associated metastasis of 4T1 breast cancer cell through anti-inflammatory property. Int J Mol Sci 17: 2109, 2016.
37. Monkkonen T and Debnath J: Inflammatory signaling cascades and autophagy in cancer. Autophagy 14: 190-198, 2018.
38. Zhao S, Shen W, Du R, Luo X, Yu J, Zhou W, Dong X, Gao R, Wang C, Yang H and Wang S: Three inflammation-related genes could predict risk in prognosis and metastasis of patients with breast cancer. Cancer Med 8: 593-605, 2019.
39. Lu Z, Long Y, Li J, Li J, Ren K, Zhao W, Wang X, Xia C, Wang Y, Li M, *et al*: Simultaneous inhibition of breast cancer and its liver and lung metastasis by blocking inflammatory feed-forward loops. J Control Release 338: 662-679, 2021.
40. Johnson DE, O'Keefe RA and Grandis JR: Targeting the IL-6/JAK/STAT3 signalling axis in cancer. Nat Rev Clin Oncol 15: 234-248, 2018.
41. Liang M, Chen X, Wang L, Qin L, Wang H, Sun Z, Zhao W and Geng B: Cancer-derived exosomal TRIM59 regulates macrophage NLRP3 inflammasome activation to promote lung cancer progression. J Exp Clin Cancer Res 39: 176, 2020.
42. Wang H, Luo Q, Feng X, Zhang R, Li J and Chen F: NLRP3 promotes tumor growth and metastasis in human oral squamous cell carcinoma. BMC Cancer 18: 500, 2018.
43. Shao X, Lei Z and Zhou C: NLRP3 promotes colorectal cancer cell proliferation and metastasis via regulating epithelial mesenchymal transformation. Anticancer Agents Med Chem 20: 820-827, 2020.
44. Deng Q, Geng Y, Zhao L, Li R, Zhang Z, Li K, Liang R, Shao X, Huang M, Zuo D, *et al*: NLRP3 inflammasomes in macrophages drive colorectal cancer metastasis to the liver. Cancer Lett 442: 21-30, 2019.
45. Lee HE, Lee JY, Yang G, Kang HC, Cho YY, Lee HS and Lee JY: Inhibition of NLRP3 inflammasome in tumor microenvironment leads to suppression of metastatic potential of cancer cells. Sci Rep 9: 12277, 2019.